

Experimental and Numerical Investigation of Non-reacting Flow in Can Combustor for Microgas Turbine Engine



V. Kirubakaran and David S. Bhatt

Abstract Generally, microgas turbines are in the range of 30–200 kW. So, here it is proposed to develop a microgas turbine engine with a capacity of 3 kW which will have applications in unmanned aerial vehicle (UAV) and standalone power generation for domestic use. In this study, the behavior of non-reacting flow pattern inside a swirl stabilized can combustor is studied. Total pressure loss, which is an important performance parameter, is predicted numerically and compared with that from experiments. Good agreement is achieved between experimental and numerical results. The combustor total pressure drop was found to be negligible; in the range of 0.002–0.06% at an inlet velocity ranges from 1.7 to 10.19 m/s. Flow pattern indicates strong vortex formation due to secondary air entrainment inside the flame tube.

Keywords CFD · Can combustor · Total pressure loss

1 Introduction

The microgas turbines are more suitable for compact power generation; the engines are classified on power ranges less than 200 kW. It has advantages futures like high power density, fuel flexibility, low emission, less maintenance and operational costs [1–4]. In literature, more emphasis is given for the development of engines more than 30 kW. However, for domestic power generation and UAVs, small engines of capacity from 1 to 10 kW are needed. So, it is aimed to develop such an engine. At the outset, the focus is to develop a small can combustor for this type of engine. The development of microgas turbine combustor is a challenging task similar to large gas turbine combustor. The combustor is one of the important components which decide the

V. Kirubakaran · D. S. Bhatt (✉)

Department of Aeronautical Engineering, Vel Tech Rangarajan Dr. Sagunthala R&D Institute of Science and Technology, Chennai, Tamil Nadu 600062, India
e-mail: davidbhatt@gmail.com

V. Kirubakaran

e-mail: kirubakaranvijayakumar@gmail.com

© The Editor(s) (if applicable) and The Author(s), under exclusive license to Springer Nature Singapore Pte Ltd. 2021

N. Gascoïn and E. Balasubramanian (eds.), *Innovative Design, Analysis and Development Practices in Aerospace and Automotive Engineering*, Lecture Notes in Mechanical Engineering, https://doi.org/10.1007/978-981-15-6619-6_14

overall performance of an engine. The flow field inside the combustor is very complex in nature because of its turbulent flow field. The gas turbine combustor has number of sub-components like diffuser, snout, swirler, flame tube and annulus. Because of this complex flow pattern inside the combustor, there is a need for detailed non-reacting flow analysis before dealing with reacting mixture for a better understanding of combustion physics. In literature, the non-reacting flow analysis in the gas turbine combustor was carried out by numerous researches [5–13]. Among this, a notable work has been carried by Anand et al., wherein detailed 3D flow has been simulated inside an annular combustor using a 20° sector for analysis. The k- ϵ RNG model was used to model turbulence. The total pressure loss of the combustor varied from 4.41 to 9.87% for a given set of input velocity 158.8–238.20 m/s. Most of the previous studies are on a large scale combustor employed in high power gas turbines. Using the same principles, a small swirl combustor of 3 kW thermal capacity is designed. In this present study, the focus is to investigate a cold flow analysis to study the flow pattern inside the newly designed small size can combustor and measure the pressure loss.

2 Combustor Geometry

An in-house designed can combustor includes diffuser, snout, swirler, flame tube and annulus. The conical diffuser with 24.2° divergence angle is used in the present study. The snout has a divergence angle of 24.8°; the axial swirler has 8 flat vanes inclined at an angle of 45°. The flame tube has 265 mm length and 46 mm diameter; it has primary zone having 88 number of 2 mm holes arranged in 4 rows, secondary zone having 60 number of 3 mm holes arranged in 4 rows and dilution zone having 24 number of 2 mm holes arranged in 3 rows. The outer annulus has 300 mm of length with 72 and 44 mm of inlet and outlet diameter. The overall thickness of can combustor is maintained as 2 mm thickness. The dimensional detail of can combustor is given in Fig. 1.

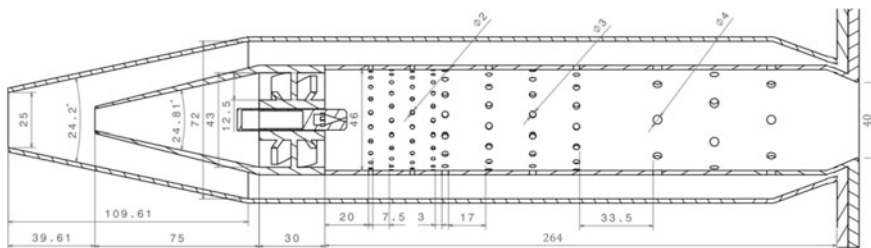


Fig. 1 Dimension details of can combustion chamber (all dimensions are in mm)

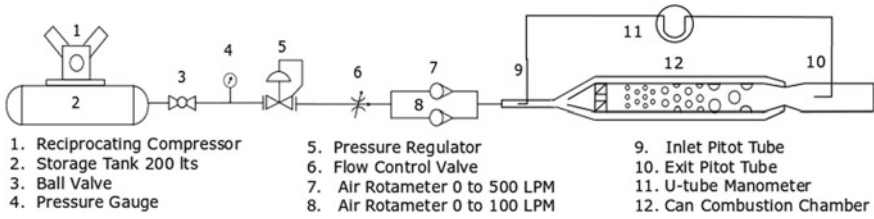


Fig. 2 Gas turbine combustor experimental setup

3 Experimental Study

The pressure loss across the combustor is measured using pitot tubes connected to a U-tube water column manometer (Fig. 2). The compressed air at 5 bar is passed through the combustor. The air mass flow rate is determined using rotameters.

4 Numerical Study

The numerical simulation is performed to predict the detailed flow field characteristics of the combustor. Here, the three-dimensional models of 90° sector are taken for analysis. The combustor flame tube wall thickness is assumed as zero, to minimize the complexity of the geometry. The turbulence modeling has been done using k-ε RNG model. The combustor inlet is specified as a velocity boundary. The outlet of the geometry is specified as a pressure outlet boundary. The inlet and outlet of snot, swirler, primary ports, secondary ports and dilution ports are specified as a interior. The sectional plane of the sector model is specified as a periodic boundary. The remaining faces of the combustor model are specified as a wall. The computational domain taken in the present study is given in Fig. 3.

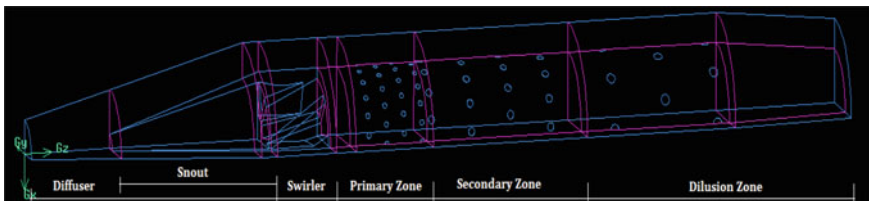


Fig. 3 90° sector can combustor computational domain

4.1 Grid-Independent Study

The unstructured grid has been employed due to the complexity of combustor geometry. The grid-independent study is carried out for four different grid sizes. The mass-weighted average of differential pressure is compared with Grid-D. The results were obtained numerically at 10.19 m/s inlet velocity. As can be seen from Table 1, almost similar results were obtained with the Grid-B and Grid-C. When grid size is increased further as in Grid-D, small difference is observed.

Alternately, the center line velocity across the combustor length for different grids (Fig. 4) is also considered. From the plot, it can be seen that the velocity profile matches closely for all grids considered. Hence, considering the optimality, Grid-B is adopted in the study.

5 Results and Discussion

The flow field inside an can combustor has been analyzed for a 90° sector model under non-reacting flow conditions. Except flame tube wall thickness, the other blockages in geometry like snout wall, swirler wall, and fuel injector were included in this analysis. The performance characteristics of the combustor for non-reacting flow

Table 1 Grid study for four different grid sizes for 10.19 m/s inlet velocity case

Description	Grid type	Elements	Differential pressure [Pa]	Difference [%]
Grid-A	Tetrahedral	2,018,026	51.90	4
Grid-B	Tetrahedral	2,687,636	48.81	2
Grid-C	Tetrahedral	4,009,738	48.37	2
Grid-D	Tetrahedral	5,942,049	46.03	–

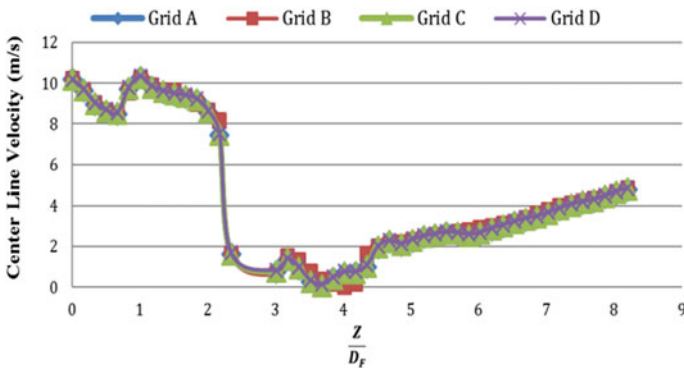


Fig. 4 Combustor center line velocity variation for 10.19 m/s inlet velocity

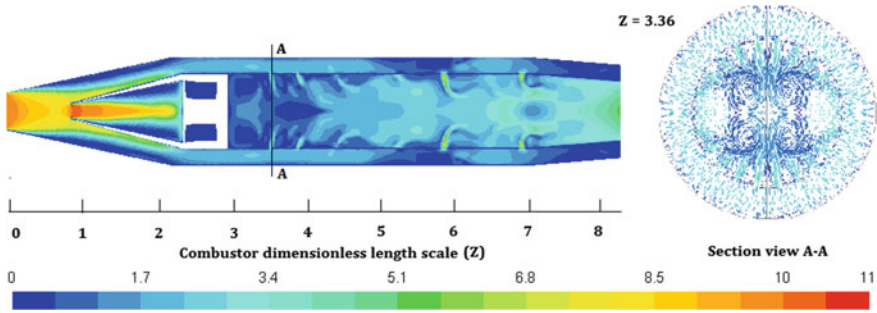


Fig. 5 Contour of velocity magnitude for inlet velocity of 10.19 m/s case

conditions with inlet velocity ranges from 1.7 to 10.19 m/s with corresponding to a Reynolds number of 2874–17,243 were evaluated.

5.1 Velocity Distribution Inside the Combustor

Figure 5 shows the reconstructed velocity contour along the length of the combustor on the symmetric plane of the 90° sector combustor. As the compressed air enters the diffuser, the flow decelerates due to area enlargement. Further, when the flow reaches the snout, the amount of air entering the snout accelerates and further decelerates due to area enlargement. Alternately, the secondary flow also decelerates due to constriction caused due to liner and blockage at the exit. When flow passes through swirler, a sudden decrease in axial velocity of the flow is seen (Fig. 4), because the swirler converts the axial component of velocity to radial and tangential components. The swirling flow helps the flame stabilize by creating a recirculation zone in the downstream. Past the swirler, the secondary air enters the combustion chamber via three zones: primary, secondary and dilution zone. The velocity of entrainment is so high that it creates a strong vortex as seen from the vector plot along the cross-section A-A at $z = 3.36$ (Fig. 5). This rotational flow would be useful in stabilizing the flame even at ultra-lean mixtures. Further downstream, as the entrainment from subsequent ports increases the net mass flow, which increases flow velocity.

5.2 Total Pressure Loss Along the Combustor

The total pressure loss across the combustor is calculated from the numerical simulation for 16 cases having velocities in the range of 1.7–10.19 m/s. These results are shown in Fig. 6 along with values obtained from the experimental study. It is seen that the pressure loss increases linearly with inlet mass flow from 0.002 to 0.06%

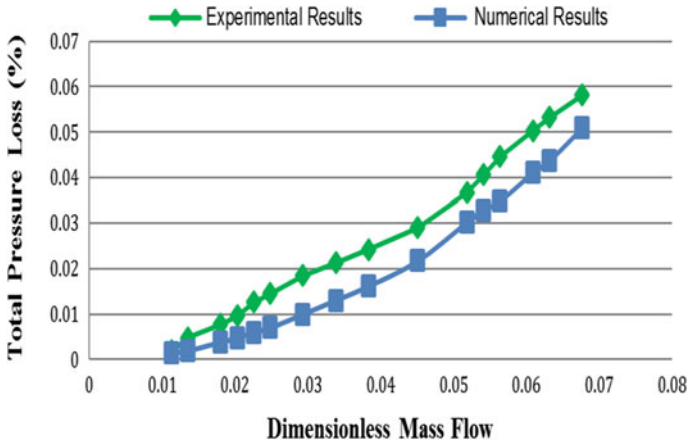


Fig. 6 Total pressure loss of combustor for various non-dimensional mass flow

as velocity is varied from 1.7 to 10.19 m/s. The good agreement found between experimental and numerical results.

6 Conclusions

The typical non-reacting flow inside the can combustor is studied experimentally as well as numerically. A swirler creates a strong recirculation zone due to the effect of radial pressure and the interaction of opposing primary jets. This would create a strong mixing of air and fuel and achieve a distributed flame region inside the combustor. The flame is also expected to be stabilized even at low equivalence ratio. The combustor total pressure drop was found to be negligible; in the range of 0.002–0.06% at an inlet velocity drop from 1.7 to 10.19 m/s. As the inlet mass flow is increased, the total pressure loss across the combustor also increases.

References

1. Xiao G, Yang T, Liu H, Ni D, Ferrari ML, Li M, Luo Z, Cen K, Ni M (2017) Recuperators for micro gas turbines: a review. *Appl Energy* 197:83–99
2. Pilavachi PA (2014) Mini- and micro-gas turbines for combined heat and power. *Appl Therm Eng* 22(18)
3. Chiamonti D, Rizzo AM, Spadi A, Prussi M, Riccio G, Martelli F (2013) Exhaust emissions from liquid fuel micro gas turbine fed with diesel oil, biodiesel and vegetable oil. *Appl Energy* 101:349–356
4. Malmquist A (2016) Modeling and simulation of an externally fired micro-gas turbine for standalone polygeneration application. *J Eng Gas Turbines Power* 138:1–15

5. Hall BF, Chana KS, Povey T (2013) Design of a non-reacting combustor simulator with swirl and temperature distortion with experimental validation. In: Proceedings of the ASME turbo expo: turbine technical conference and exposition. Volume 3C: heat transfer. San Antonio, Texas, USA. June 3–7, 2013. V03CT17A010. ASME
6. Gouda P, Srinivasan K, Sivaramakrishna G, Shashishekar KS (2016) CFD analysis of gas turbine combustor primary zone using different axial swirler configurations. *Int J Mech Prod Eng* 4(6)
7. Karuppanan S, Sondur VM, Sivaramakrishna G, Navindgi RD, Muthuveerappan N (2017) CFD analyses of combustor-diffuser system of marine gas turbine engine. In: Proceedings of the ASME gas turbine india conference. Volume 1: compressors, fans and pumps; turbines; heat transfer; combustion, fuels and emissions. Bangalore, India. V001T04A013. ASME
8. Crocker DS, Nickolaus D, Smith CE (1999) CFD modeling of a gas turbine combustor from compressor exit to turbine inlet. *ASME J Eng Gas Turbines Power* 121(1), 89–95
9. Ananda Reddy G, Ganesan V (2004) Non-reacting flow analysis from combustor inlet to outlet using computational fluid dynamics code. *Defence Sci J* 54(4), 455–467
10. Dzida M, Kosowski K (2015) Experimental investigations of pressure drop in the combustion chamber of gas turbine. ASME. Turbo expo: power for land, sea, and air. Volume 3: coal, biomass and alternative fuels; combustion and fuels; oil and gas applications. V003T06A001
11. Knight MA, Walker RB (1957) The component pressure losses in combustion chambers. Aeronautical Research Council R and M 2987, UK
12. Zhou D, Wang T (1998) Cold flow computations for the diffuser-combustor section of an industrial gas turbine. ASME 96-GT-513, Presented at the international gas turbine and aero engine congress and exhibition, Birmingham, UK
13. Lefebvre AH, Ballal DR (2010) Gas turbine combustion